

Effect of spin ordering on the magnetotransport of $\text{YBa}_2\text{Cu}_3\text{O}_{6.25}$

E. Cimpoiasu, V. Sandu,* and C. C. Almasan
Department of Physics, Kent State University, Kent, Ohio 44242

A. P. Paulikas and B. W. Veal

Materials Science Division, Argonne National Laboratory, Argonne, Illinois 60439

(Received 17 September 2001; revised manuscript received 29 November 2001; published 25 March 2002)

In-plane and out-of-plane magnetoresistivity (MR) measurements were performed on the same antiferromagnetic (AF) $\text{YBa}_2\text{Cu}_3\text{O}_{6.25}$ single crystal using a six-lead configuration, in magnetic fields H applied along the ab plane. We identified three terms contributing to both MRs. The first term is anisotropic with respect to the in-plane field orientation, with a twofold symmetry for the in-plane MR and a fourfold symmetry for the out-of-plane MR. We show that these anisotropic features of the magnetoresistivity tensor can be understood in terms of the coupling between the spin and the elastic degrees of freedom. The second term in both MRs is negative and isotropic upon in-plane H rotation. We ascribe this term to charge-carrier scattering on the AF domain walls. Finally, the third term is positive, quadratic in H and seems to correlate with the AF phase transition.

DOI: 10.1103/PhysRevB.65.144505

PACS number(s): 74.25.Fy, 74.72.Bk

I. INTRODUCTION

The interplay between the charge and spin subsystems plays a central role in the physics of high-temperature superconductors. This interplay, tuned by charge doping, underlies the dramatic changes in the physical properties across the phase diagram of these materials. Here, we focus on the electronic transport properties of antiferromagnetic (AF) $\text{YBa}_2\text{Cu}_3\text{O}_x$ in order to better understand the effect of spin ordering on electrical conduction.

Charge transport in antiferromagnetic $\text{YBa}_2\text{Cu}_3\text{O}_x$ single crystals exhibits unusual features in the presence of a magnetic field H applied parallel to the ab planes.^{1,2} Namely, the in-plane magnetoresistivity (MR) $\Delta\rho_{ab}/\rho_{ab} \equiv [\rho_{ab}(H) - \rho_{ab}(H=0)]/\rho_{ab}$ is anisotropic with respect to the relative orientation between the electrical current I and the applied magnetic field, changing from positive when $H \perp I$ to negative when $H \parallel I$. Also, the field dependence of $\Delta\rho_{ab}/\rho_{ab}$ increases sharply in low H and shows signs of saturation above a certain threshold field, where it varies slowly with H .

There are three main scenarios put forward to explain the unusual behavior of the in-plane magnetoresistivity. The first scenario invokes the segregation of charges within an array of stripes.¹ These stripes align along the direction of the magnetic field as a result of their ferromagnetic coupling with H . Consequently, $\Delta\rho_{ab}/\rho_{ab} < 0$ for $H \parallel I$ and $\Delta\rho_{ab}/\rho_{ab} > 0$ for $H \perp I$. The second scenario invokes the presence of an in-plane orthorhombic distortion of the crystal lattice in the AF state due to its coupling with the antiferromagnetically ordered Cu(2) magnetic moments.³ This leads to an in-plane anisotropy of the bulk resistivities: resistivity is larger when I is parallel to the sublattice magnetization and smaller when I is perpendicular to the sublattice magnetization. An average resistivity is measured in the absence of a magnetic field. Since the sublattice magnetization in high fields is perpendicular to H , $\Delta\rho_{ab}/\rho_{ab} < 0$ for $H \parallel I$ and $\Delta\rho_{ab}/\rho_{ab} > 0$ for $H \perp I$. Moskvin and Panov proposed a third scenario in which the features of the in-plane MR are linked

to the spin-induced orbital polarization of the triplet state of oxygen in the CuO_4 centers.⁴

We present here systematic angle- and temperature-dependent in-plane and out-of-plane MR measurements, performed simultaneously on the same single crystal by using a six-lead configuration technique,⁵ with the magnetic field H applied parallel to the ab planes. Motivated by the experimental evidence for the spin-lattice coupling in these AF compositions,⁶ we determine here the effect of the lattice distortions on the MR tensor. We further estimate the magnitude of this effect and identify the features of the MRs that can be explained on the basis of the magnetostriction effect. We also show that the asymmetry observed in the saturation regime in the $\Delta\rho_{ab}/\rho_{ab}(H)$ curves, when $H \perp I$ and $H \parallel I$, vanishes for temperatures higher than the Néel transition temperature T_N and is consistent with a transport mechanism involving charge-carrier scattering on the AF domain walls (DW). This asymmetry also correlates with the negative contribution to the out-of-plane MR measured under the same field orientations at $T > 100$ K, indicating that a common mechanism is responsible for both behaviors.

II. EXPERIMENTAL DETAILS

Single crystals of antiferromagnetic $\text{YBa}_2\text{Cu}_3\text{O}_{6.25}$ were grown in gold crucibles using the self-flux method. The oxygen stoichiometry was adjusted by annealing the samples at 500 °C in a predetermined $\text{O}_2\text{-N}_2$ atmosphere, followed by a quench to liquid-nitrogen temperature. The oxygen partial pressure P_{O_2} , in atmospheres, was determined from the equation $\ln(P_{\text{O}_2}) = A + Bx$, where $A = -96.26$, $B = 13.96$, and x is the desired oxygen stoichiometry of the single crystal.⁷ Typical dimensions are $0.8 \times 0.5 \times 0.04$ mm³ with the c axis of the single crystals oriented along the smallest dimension.

We have used a multiterminal lead configuration for the simultaneous measurement of the in-plane ρ_{ab} and out-of-

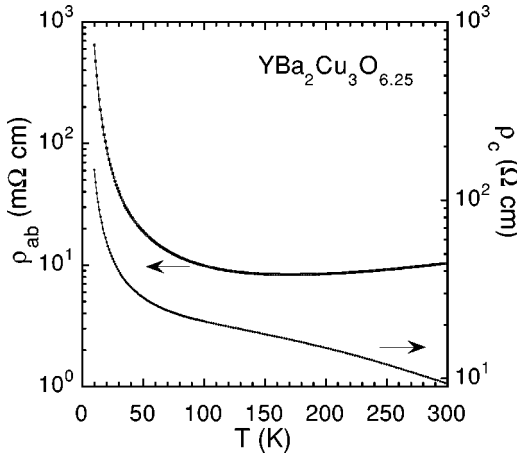


FIG. 1. Temperature T dependence of the zero-field in-plane, ρ_{ab} , and out-of-plane, ρ_c , resistivities of $\text{YBa}_2\text{Cu}_3\text{O}_{6.25}$ single crystal.

plane ρ_c resistivities and the respective magnetoresistivities $\Delta\rho_{ab}/\rho_{ab}$ and $\Delta\rho_c/\rho_c$. A total of eight low-resistance electrical contacts are applied on the top and bottom faces of the crystal using thermally treated silver pads and room-temperature silver epoxy. The electrical current I is always applied along one of the crystal faces, while the top and bottom face voltages are measured simultaneously. A mathematical algorithm is subsequently used to extract the two components of the resistivity tensor.⁸ The MR measurements were performed at constant temperature T in sweeping H up to 14 T applied along the ab planes ($H\parallel ab$). The angular dependence of MR was determined by rotating the sample between 0° and 360° in constant H and T .

During measurements, special care was taken to account for the magnetoresistance of the temperature sensors (Pt or Cernox) and to eliminate the contribution of the Hall effect to the measured voltages.⁹ We checked the quality of our samples by performing multiterminal measurements with different lead configurations in zero field while sweeping T between $10\text{ K} \leq T \leq 300\text{ K}$. Samples free of defects and inhomogeneities should yield identical resistivity values when measured using different lead configurations. The single crystal for which data are shown here has less than 10% change in resistivity when measured using different lead configurations.

III. RESULTS

Typical $\rho_{ab}(T)$ and $\rho_c(T)$ ($10\text{ K} \leq T \leq 300\text{ K}$) for $\text{YBa}_2\text{Cu}_3\text{O}_{6.25}$ are shown in Fig. 1. For $175\text{ K} \leq T \leq 300\text{ K}$, $\rho_{ab}(T)$ is weakly metallic despite the fact that the sample is strongly underdoped. $\rho_{ab}(T)$ exhibits two crossovers with decreasing T : a crossover from metallic to weak localization behavior at 175 K and a second crossover to two-dimensional variable-range hopping (VRH) of localized holes in a textured magnetic system at 115 K.¹⁰ In contrast, $\rho_c(T)$ is very large and displays a nonmetallic behavior over the whole T range with a VRH-type dependence below 115 K.¹⁰ The kink in the T derivative of ρ_c , which occurs while cooling through T_N ,¹¹ was not detected for the measured T

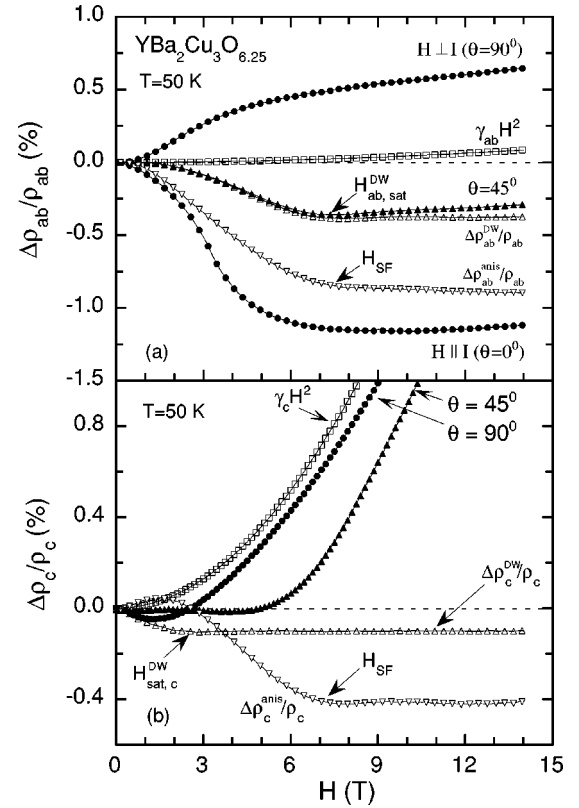


FIG. 2. Field H dependence of (a) in-plane magnetoresistivity $\Delta\rho_{ab}/\rho_{ab}$ and (b) out-of-plane magnetoresistivity $\Delta\rho_c/\rho_c$ of $\text{YBa}_2\text{Cu}_3\text{O}_{6.25}$ single crystal measured at 50 K with different field orientations (filled symbols). The filled circles correspond to $H\parallel I\parallel ab$ plane and $H\perp I$, while the filled triangles correspond to $\theta = 45^\circ$. The three curves shown with empty symbols are extracted from the raw data (filled symbols) as follows. The anisotropic term $\Delta\rho_{ab,c}^{anis}/\rho_{ab,c}$ (inverted triangles) is the difference between $\Delta\rho_{ab,c}/\rho_{ab,c}(H,0^\circ)$ and $\Delta\rho_{ab,c}/\rho_{ab,c}(H,45^\circ)$, while the quadratic in H term $\gamma_{ab,c}H^2$ (squares) was subtracted from $\Delta\rho_{ab}/\rho_{ab}(H,45^\circ)$ and $\Delta\rho_c/\rho_c(H,90^\circ)$, respectively, to, hence, give the term attributed to domains-wall scattering, $\Delta\rho_{ab,c}^{DW}/\rho_{ab,c}$ (open triangles). Thus, the sum of the three curves shown with empty symbols gives $\Delta\rho_{ab}/\rho_{ab}(H,0^\circ)$ and $\Delta\rho_c/\rho_c(H,45^\circ)$, respectively.

range, indicating that $T_N > 300\text{ K}$.

There are several unusual features that characterize the magnetotransport of these low oxygen concentrations in magnetic field H applied parallel to the CuO_2 planes. First, the H dependence of $\Delta\rho_{ab,c}/\rho_{ab,c}$ is a superposition of three contributions. Figure 2(a) illustrates the H dependence of $\Delta\rho_{ab}/\rho_{ab}$ measured at $T = 50\text{ K}$ at three different angles: 0° and 90° (filled circles), and 45° (filled triangles). Here $\theta = 0^\circ$ corresponds to H parallel to the x axis (defined along the longest dimension of the single crystal), which corresponds to the direction of I and to one of the in-plane crystallographic axes $a(b)$. Note that $\Delta\rho_{ab}/\rho_{ab}$ is strongly anisotropic, i.e., $\Delta\rho_{ab}/\rho_{ab}$ is negative when $H\parallel I$ ($\theta = 0^\circ$) and is positive when $H\perp I$ ($\theta = 90^\circ$). The $\Delta\rho_{ab}/\rho_{ab}(H)$ curves corresponding to these two field-current configurations are almost symmetric with respect to the $\Delta\rho_{ab}/\rho_{ab}(H)$ curve corresponding to the $\theta = 45^\circ$ configuration. Hence, there is

an anisotropic contribution $\Delta\rho_{ab}^{anis}/\rho_{ab}(H,\theta)$, given by the difference between $\Delta\rho_{ab}/\rho_{ab}(H,\theta)$ and $\Delta\rho_{ab}/\rho_{ab}(H,45^\circ)$. The H dependence of $\Delta\rho_{ab}^{anis}/\rho_{ab}$ for $\theta=0^\circ$ is shown in Fig. 2(a) (inverted triangles). This term is strongly H dependent for low H and saturates for H higher than a certain value H_{SF} . Thus, $\Delta\rho_{ab}/\rho_{ab}(H,\theta)$ is the sum of two terms: $\Delta\rho_{ab}/\rho_{ab}(H,45^\circ)$ and $\Delta\rho_{ab}^{anis}/\rho_{ab}(H,\theta)$. The $\Delta\rho_{ab}/\rho_{ab}(H,45^\circ)$ term is also a superposition of two contributions: (i) a positive, isotropic, and quadratic in H contribution, $\gamma_{ab}H^2$ [open squares in Fig. 2(a)], and (ii) a negative contribution $\Delta\rho_{ab}^{DW}/\rho_{ab}$ (open triangles), which increases sharply with H at low H and saturates for magnetic fields higher than a threshold value $H_{ab,sat}^{DW}$.

A similar superposition of three different terms is also characteristic to the H dependence of $\Delta\rho_c/\rho_c$. Figure 2(b) illustrates the H dependence of $\Delta\rho_c/\rho_c$ measured at $T=50$ K with $\theta=90^\circ$ (filled circles) and $\theta=45^\circ$ (filled triangles). The results for $\theta=0^\circ$ (data not shown) are almost identical with the results for $\theta=90^\circ$, as expected from symmetry reasons. The $\Delta\rho_c/\rho_c(H,45^\circ)$ and $\Delta\rho_c/\rho_c(H,90^\circ)$ curves differ by a term $\Delta\rho_c^{anis}/\rho_c(H,45^\circ)$ (inverted triangles). Thus, there is an anisotropic term $\Delta\rho_c^{anis}/\rho_c(H,\theta)$ contributing to the c -axis MR, given by the difference between $\Delta\rho_c/\rho_c(H,\theta)$ and $\Delta\rho_c/\rho_c(H,90^\circ)$. This $\Delta\rho_c^{anis}/\rho_c$ term increases with H for low H and saturates for $H > H_{SF}$, with H_{SF} the same for both $\Delta\rho_{ab}^{anis}/\rho_{ab}$ and $\Delta\rho_c^{anis}/\rho_c$. Thus, similarly to the in-plane MR, $\Delta\rho_c/\rho_c(H,\theta)$ is the sum of two terms $\Delta\rho_c/\rho_c(H,90^\circ)$ and $\Delta\rho_c^{anis}/\rho_c(H,\theta)$. The $\Delta\rho_c/\rho_c(H,90^\circ)$ term is also a superposition of two contributions: (i) a positive, isotropic, and quadratic in H contribution, $\gamma_c H^2$, dominant at high H (open squares) and (ii) a negative contribution $\Delta\rho_c^{DW}/\rho_c(H)$ (open triangles), which increases sharply with H at low H and saturates for magnetic fields higher than a threshold value $H_{c,sat}^{DW}$.

As anticipated from above, the MRs are strongly anisotropic upon the in-plane rotation of H . This feature is best illustrated in the angular dependence of $\Delta\rho_{ab,c}/\rho_{ab,c}$ measured at constant T . Figure 3(a) is a plot of $\Delta\rho_{ab}^{anis}/\rho_{ab}$ vs θ . Notice that $\Delta\rho_{ab}^{anis}/\rho_{ab}$ has a twofold symmetry and an enhancing anisotropy with decreasing T . The angular dependence of $\Delta\rho_c^{anis}/\rho_c$ is shown in Fig. 3(b). This term exhibits a fourfold symmetry, with minima at 45° between H and $a(b)$. Its anisotropy is again enhanced with decreasing T .

We show next that the anisotropic features of $\Delta\rho_{ab,c}/\rho_{ab,c}$ at high H values can be understood in terms of the coupling between the spin and elastic degrees of freedom in the antiferromagnetic state, with the a and b directions corresponding to the easy axes of magnetization. We also show that the asymmetry of the $\Delta\rho_{ab}/\rho_{ab}(H)$ curves when $H\parallel I$ and $H\perp I$, i.e., the $\Delta\rho_{ab}^{DW}/\rho_{ab}$ term, as well as the negative contribution to $\Delta\rho_c/\rho_c$, i.e., the $\Delta\rho_c^{DW}/\rho_c$ term, may be the result of charge-carrier scattering on the antiferromagnetic domain walls.

IV. EFFECT OF LATTICE DISTORTIONS ON MAGNETOTRANSPORT

Below T_N , the spins of the Cu ions are oriented along the CuO_2 planes and are antiferromagnetically ordered both in-

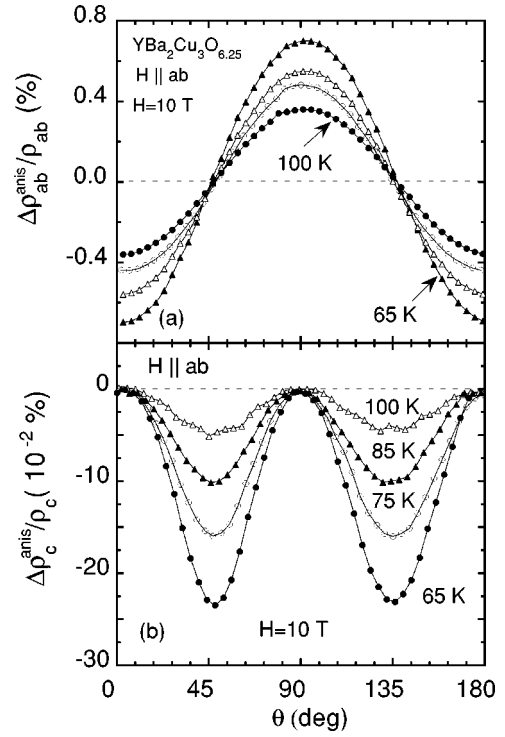


FIG. 3. Angular θ dependence of (a) the in-plane $\Delta\rho_{ab}^{anis}/\rho_{ab}$ and (b) out-of-plane $\Delta\rho_c^{anis}/\rho_c$ anisotropic contributions to the magnetoresistivities of $\text{YBa}_2\text{Cu}_3\text{O}_{6.25}$ single crystal measured at different temperatures T in a magnetic field $H=10$ T applied parallel to the ab plane. θ is the angle between H and the applied current I with $\theta=0^\circ$ when $H\parallel I$. The direction of I is along the crystallographic axis a (b).

plane and out of the plane.¹² The single crystal is divided into antiferromagnetic domains. In each domain, the sublattice magnetizations \mathbf{M}_1 and \mathbf{M}_2 with $M_1=M_2=M_s$ are antiparallel to each other, with the staggered magnetization $\mathbf{L}=\mathbf{M}_1-\mathbf{M}_2$ oriented along the easy axes of magnetization. In the absence of an applied magnetic field, the orientation of the domains is equally distributed between the two easy axes of magnetization. When the magnetic field is increased from $H=0$, the domains with unfavorably oriented sublattice magnetizations rotate perpendicular to the direction of H and, for a value of H higher than a threshold value H_{SF} , the system reaches the single-domain state. In $H>H_{SF}$, the sublattice magnetizations are canted relative to each other, towards the direction of the field, and the total magnetization $\mathbf{M}=\mathbf{M}_1+\mathbf{M}_2$ becomes different than zero. The canting angle increases with increasing field up to a maximum field H_E , when all the spins are aligned along the direction of H .

Upon the onset of long-range antiferromagnetic ordering, the crystal lattice is slightly distorted along the direction of \mathbf{L} (magnetostriction) as a result of its coupling with the antiferromagnetically ordered $\text{Cu}(2)$ spins. Thus, inside each antiferromagnetic domain, the crystal symmetry is lowered from tetragonal to orthorhombic, giving rise to a nonzero strain tensor e_{ij} and to a change in the in-plane and out-of-plane resistivities. This spin-lattice coupling was experimentally confirmed for antiferromagnetic $\text{YBa}_2\text{Cu}_3\text{O}_{6.1}$ single crystals

doped with 1% Gd through electron-spin-resonance measurements.⁶

In determining the effect of the lattice distortions on ρ_{ab} and ρ_c , we start with the assumption that both ρ_{ab} and ρ_c are functions of the diagonal components e_{xx} , e_{yy} , and e_{zz} of the strain tensor, produced by the magnetoelastic coupling. We write both resistivities as a power series of isotropic $\Sigma = e_{xx} + e_{yy} + e_{zz}$ and anisotropic $\Delta = e_{xx} - e_{yy}$ combinations of the strains since, for axial symmetry, the component e_{zz} is a function of the sum $e_{xx} + e_{yy}$.¹³ Hence, to second order in Σ and Δ , the resistivities are given by

$$\rho_{ab} = \rho_{0,ab} + a_{p1}\Sigma + b_{p1}\Delta + a_{p2}\Sigma^2 + b_{p2}\Delta^2, \quad (1)$$

$$\rho_c = \rho_{0,c} + a_{c1}\Sigma + a_{c2}\Sigma^2 + b_c\Delta^2. \quad (2)$$

Here $\rho_{0,ab}$ and $\rho_{0,c}$ are resistivities due to scattering mechanisms unrelated to lattice distortions, while $a_{p1,p2}$, $b_{p1,p2}$, $a_{c1,c2}$, and b_c are material dependent coefficients. The ρ_c expansion does not include a linear term in Δ because of the symmetry of the crystalline structure and the experimental configuration.

The choice to expand ρ_c and ρ_{ab} in a power series of Δ and Σ is a natural one. For instance, the relative change of the volume (Σ) is expected to affect both in-plane and out-of-plane hopping integrals $t_{\parallel} = \hbar/(2m_{\parallel}^*a^2)$ and $t_{\perp} = \hbar/(2m_{\perp}^*c^2)$ and, therefore, to produce a change in ρ_c and ρ_{ab} . However, the relative change in volume does not scale with the change in resistivities;^{14–17} hence, Σ is not the only source for the change in ρ_{ab} and ρ_c . Indeed, experiments have shown that lattice deformations produce a change in both the transport hopping integrals and charge-carrier density.^{18–20} Specifically, the charge-carrier density was found to increase under compression. This increase was ascribed to an enhanced chain ordering upon volume reduction²¹ and, from a crystallographic point of view, to an enhanced orthorhombicity $(a-b)/a$. (The Hall number, which is related to the charge-carrier density, does not change under pressure in systems without Cu-O chains.²²) Based on these results, we expect the change in the orthorhombicity $[(a-b)/a \propto e_{xx} - e_{yy} \propto \Delta]$ of the $\text{YB}_2\text{Cu}_3\text{O}_{6.25}$ sample, produced by spin-lattice coupling, to also induce a change in the charge-carrier density, thus affecting both ρ_{ab} and ρ_c .

The strains e_{ii} ($i=x,y,z$) are obtained starting from the total free energy of the antiferromagnetic sample in the single-domain state ($H > H_{SF}$). To second-order approximation and for a crystallographic lattice with tetragonal symmetry, the free energy can be written as²³

$$\begin{aligned} F = & \frac{1}{2}A l^2 + \frac{1}{2}B m^2 + \frac{1}{2}K_2 l_x^2 l_y^2 - 2M_s \mathbf{m} \cdot \mathbf{H} + B_{11}(e_{xx} l_x^2 + e_{yy} l_y^2) \\ & + B_{12}(e_{xx} l_y^2 + e_{yy} l_x^2) + B_{31} l^2 e_{zz} + 2B_{66} e_{xy} l_x l_y \\ & + \frac{1}{2}C_{11}(e_{xx}^2 + e_{yy}^2) + C_{12} e_{xx} e_{yy} + C_{13}(e_{xx} + e_{yy}) e_{zz} \\ & + \frac{1}{2}C_{33} e_{zz}^2 + 2C_{44}(e_{xz}^2 + e_{yz}^2) + 2C_{66} e_{xy}^2. \end{aligned} \quad (3)$$

The first four terms represent the magnetic interaction (two exchange terms, an anisotropy term, and a Zeeman term, respectively) expressed in terms of reduced staggered mag-

netization $\mathbf{l} = \mathbf{L}/(2M_s)$ and reduced magnetization $\mathbf{m} = \mathbf{M}/(2M_s)$. The next four terms represent the magnetoelastic energies with magnetoelastic constants B_{ij} . The last six terms represent the elastic energy with elastic constants C_{ij} . With the x axis along one of the equivalent in-plane crystallographic axes $a(b)$, we define α and θ as the angles between the x axis and \mathbf{l} and \mathbf{H} , respectively, $h = H/(2M_s)$ as the reduced magnetic field, and β by $l = \cos \beta$ and $m = \sin \beta$. With these definitions, the free energy becomes

$$\begin{aligned} F = & \frac{1}{2}(A - B)\cos^2 \beta - \frac{1}{16}K_2 \cos^4 \beta \cos 4\alpha \\ & - 2M_s h \sin \beta \sin(\alpha - \theta) + \frac{1}{2}\cos^2 \beta [(B_{11} - B_{12}) \\ & \times (e_{xx} - e_{yy}) \cos 2\alpha + (B_{11} + B_{12})(e_{xx} + e_{yy}) \\ & + 2B_{31} e_{zz} + 2B_{66} e_{xy} \sin 2\alpha] + \frac{1}{2}C_{11}(e_{xx}^2 + e_{yy}^2) \\ & + C_{12} e_{xx} e_{yy} + C_{13}(e_{xx} + e_{yy}) e_{zz} + \frac{1}{2}C_{33} e_{zz}^2 \\ & + 2C_{44}(e_{xz}^2 + e_{yz}^2) + 2C_{66} e_{xy}^2. \end{aligned} \quad (4)$$

The minimization of the free energy with respect to α , β , and e_{ij} ($i,j=x,y,z$) gives β and the strains e_{ij} as functions of h . The expressions of β and of the isotropic and anisotropic strains are

$$\sin \beta \equiv m = \frac{h}{h_E} \sin(\alpha - \theta), \quad (5)$$

$$\Sigma = -C_m \cos^2 \beta, \quad (6)$$

$$\Delta = -D_m \cos 2\alpha \cos^2 \beta, \quad (7)$$

where $h_E \equiv H_E/(2M_s) = (B - A)/(2M_s^2)$ is the reduced exchange field, and C_m and D_m are T -dependent magnetoelastic factors defined as

$$C_m = \frac{B_{11} + B_{12} - 2B_{31} \frac{C_{13}}{C_{33}}}{C_{11} + C_{12} - 2 \frac{C_{13}^2}{C_{33}}} \left(1 - \frac{C_{13}}{C_{33}} \right) + \frac{B_{31}}{C_{33}},$$

$$D_m = \frac{B_{11} - B_{12}}{C_{11} - C_{12}}. \quad (8)$$

The minimization of the free energy also gives the angle α ,

$$\sin 4\alpha = 2 \left(\frac{h}{h_{SF}} \right)^2 \sin 2(\alpha - \theta), \quad (9)$$

where $h_{SF} \equiv H_{SF}/(2M_s) = \sqrt{K_2'(B - A)}/(2M_s^2)$ is the reduced spin-flop field with the renormalized anisotropy constant

$$K'_2 = K_2 + 2 \frac{(B_{11} - B_{12})^2}{C_{11} - C_{12}} - \frac{B_{66}^2}{C_{66}}. \quad (10)$$

For fields higher than H_{SF} , Eq. (9) has the solution $\alpha = \pi/2 + \theta + \delta$, with

$$\delta \approx - \frac{\sin 4\theta}{4 \left[\left(\frac{h}{h_{SF}} \right)^2 + \cos 4\theta \right]} \ll 1. \quad (11)$$

This means that, for $H > H_{SF}$, the staggered magnetization is nearly always perpendicular to the direction of the magnetic field and rotates simultaneously with the magnetic field, but with an approximately $\pi/2$ phase shift.

Inserting Eqs. (6) and (7) into Eqs. (1) and (2), and with $\cos^2 \beta \approx 1 - h^2/h_E^2$ one obtains the following field and angular dependences of ρ_{ab} (expressed up to first order in Σ and Δ) and ρ_c (expressed up to second order in Σ and Δ):

$$\begin{aligned} \rho_{ab}(H) &= \rho_{0,ab}(H) - a_{p1} C_m \left[1 - \left(\frac{H}{H_E} \right)^2 \right] \\ &\quad + b_{p1} D_m \left[1 - \left(\frac{H}{H_E} \right)^2 \right] \cos 2\theta, \\ \rho_c(H) &= \rho_{0,c}(H) - a_{c1} C_m \left[1 - \left(\frac{H}{H_E} \right)^2 \right] \\ &\quad + a_{c2} C_m^2 \left[1 - 2 \left(\frac{H}{H_E} \right)^2 \right] \\ &\quad + \frac{b_c D_m^2}{2} \left[1 - 2 \left(\frac{H}{H_E} \right)^2 \right] (1 + \cos 4\theta). \end{aligned} \quad (12)$$

In order to determine the magnetoresistivities, it is necessary to know the zero-field values of Σ and Δ that enter in the expressions of ρ_{ab} and ρ_c for $H=0$ T. These values can be evaluated starting from the expression of the free energy, i.e., Eq. (3), without the terms due to the magnetic field [second and fourth terms of Eq. (3)]. The minimization of the free energy leads to two solutions for the angle α : $\alpha=0$ and $\pi/2$. This indicates that at $H=0$ T, the sample splits into antiferromagnetic domains, which, for a perfect single crystal, orient in equal numbers along the two easy axes of magnetization. Then, one gets the zero-field value of Σ and Δ by taking the average of the values obtained from Eqs. (6) and (7), respectively, with $\alpha=0$ and $\pi/2$: $\Sigma(0)_{av} = -C_m$, $\Delta(0)_{av} = 0$, $\Sigma^2(0)_{av} = C_m^2$, and $\Delta^2(0)_{av} = D_m^2$. As a result, $\Delta\rho_{ab} = \rho_{ab}(H) - \rho_{ab}(0)$ and $\Delta\rho_c = \rho_c(H) - \rho_c(0)$ are given by

$$\Delta\rho_{ab} = \Delta\rho_{0,ab} + a_{p1} C_m \left(\frac{H}{H_E} \right)^2 + b_{p1} D_m \left[1 - \left(\frac{H}{H_E} \right)^2 \right] \cos 2\theta, \quad (13)$$

$$\begin{aligned} \Delta\rho_c &= \Delta\rho_{0,c} + [a_{c1} C_m - 2a_{c2} C_m^2 - 2b_c D_m^2] \left(\frac{H}{H_E} \right)^2 \\ &\quad - \frac{b_c D_m^2}{2} \left[1 - 2 \left(\frac{H}{H_E} \right)^2 \right] (1 - \cos 4\theta), \end{aligned} \quad (14)$$

where $\Delta\rho_{0,ab} = \rho_{0,ab}(H) - \rho_{0,ab}(0)$ and $\Delta\rho_{0,c} = \rho_{0,c}(H) - \rho_{0,c}(0)$.

Equations (13) and (14) predict the existence of three terms contributing to both in-plane and out-of-plane magnetoresistivities: the first term is generated by mechanisms independent of lattice distortions, while the second and third terms are a result of lattice distortions. The second term is quadratic in field and independent of the angle between H and the crystallographic axes, while the third term is anisotropic with respect to the in-plane field orientation, with a twofold symmetry (2θ) in $\Delta\rho_{ab}$ and a fourfold symmetry (4θ) in $\Delta\rho_c$.

The angular dependences of $\Delta\rho_{ab,c}^{anis}/\rho_{ab,c}$ shown in Figs. 3(a) and 3(b), with a $\cos 2\theta$ behavior for $\Delta\rho_{ab}^{anis}/\rho_{ab}$, and $\cos 4\theta$ behavior for $\Delta\rho_c^{anis}/\rho_c$, are in excellent agreement with the angular dependences predicted by the anisotropic terms of Eqs. (13) and (14). Also, Figs. 3(a) and 3(b) show that $\Delta\rho_c^{anis}/\rho_c$ is approximately one order of magnitude smaller than $\Delta\rho_{ab}^{anis}/\rho_{ab}$. This is consistent with the fact that a second-order approximation had to be employed in order to reveal the angular behavior of $\Delta\rho_c/\rho_c$, while a first-order approximation was used for $\Delta\rho_{ab}/\rho_{ab}$.

Thus, the magnetoelastic coupling explains the unusual *angular dependence* exhibited by both MRs, and, therefore, constitutes a valid candidate for the origin of this behavior. However, in order to see if the lattice distortions account for the *magnitude* of the anisotropic term in MRs, we estimate the order of magnitude of the change in the lattice parameter and, hence, of the magnetostriction required to produce the measured magnitude of the anisotropic term in MRs and compare this estimate with known magnetostriction data. Both magnetostriction and applied pressure give rise to changes of the lattice parameters and, subsequently, to changes in resistivity. The change in resistivity as a result of uniaxial stress applied along the a axis is $\Delta\rho_{ab}/\rho_{ab} \approx -(d \ln \rho_{ab}/dp_a) \kappa_a^{-1} (\Delta a/a)$, where $\kappa_a = -d \ln a/dp_a$ and $\Delta a/a$ is the relative change in the lattice parameter a as a result of the applied uniaxial stress p_a . With $\kappa_a \approx -2.4 \times 10^{-3} \text{ GPa}^{-1}$ from Ref. 21, $d \ln \rho_{ab}/dp_a \approx -0.4 \text{ GPa}^{-1}$ from Ref. 19, and $\Delta\rho_{ab}^{anis}/\rho_{ab} \approx 10^{-3}$ from our measurements in the single-domain state, one obtains $\Delta a/a = e_{xx} \approx 6 \times 10^{-6}$. This is in good agreement with the reported values of $10^{-6} - 10^{-5}$ on magnetostriction in layered cuprates.^{24,25}

As mentioned above, Eqs. (13) and (14) also predict the presence of an H^2 term for both in-plane and out-of-plane resistivities, independent of the in-plane field orientation. The H dependence of $\Delta\rho_{ab}/\rho_{ab}$ and $\Delta\rho_c/\rho_c$ measured at constant T and fixed H orientation [see Figs. 2(a) and 2(b)] exhibits a quadratic contribution as well, which appears to be, within experimental errors, independent of field orientation.

We check next if the magnitude of the measured *isotropic*

H^2 term could be accounted for by *isotropic* forced magnetostriction alone [second terms in Eqs. (13) and (14)]. Specifically, from data of hydrostatic pressure dependence of in-plane resistivity of $\text{YBa}_2\text{Cu}_3\text{O}_{6+x}$, we estimate the magnitude of the magnetostriction necessary to induce an H^2 term in $\Delta\rho_{ab}/\rho_{ab}$ of the order of 10^{-3} at 14 T. A relative change of volume, $\Delta V/V$, produces a change in the resistivity given by $\Delta\rho_{ab}/\rho_{ab} \approx (-d \ln \rho_{ab}/dp) \kappa_V^{-1} \Delta V/V$, where p represents the applied hydrostatic pressure, $\kappa_V = -d \ln V/dp \approx -8.9 \times 10^{-3} \text{ GPa}^{-1}$, and $d \ln \rho_{ab}/dp \approx -0.12 \text{ GPa}^{-1}$ from Ref. 21. An applied magnetic field induces a relative change in volume $\Delta V/V = \Sigma(0)(H/H_E)^2$, where $\Sigma(0) = e_{xx} + e_{yy} + e_{zz}$ is the zero-field isotropic magnetostriction. With $H_E \approx 600 \text{ T}$ (see Ref. 26), one obtains $\Sigma(0) \propto 0.1$. This is an extremely large value since $\Sigma(0)$ is, at most, of the order of $3e_{xx} \approx 10^{-6} - 10^{-5}$. Therefore, we conclude that the isotropic forced magnetostriction alone [second term in Eqs. (13) and (14)] produces negligible contribution to MRs and cannot account for the measured magnitude of the *isotropic* H^2 term in $\Delta\rho_{ab}/\rho_{ab}$ and $\Delta\rho_c/\rho_c$.

V. EFFECT OF OTHER MECHANISMS ON MAGNETOTRANSPORT

We address now the contributions $\Delta\rho_{ab,0}/\rho_{ab}$ and $\Delta\rho_{c,0}/\rho_c$ in Eqs. (13) and (14), respectively, which represent mechanisms independent of lattice distortions. We note that $\Delta\rho_{ab,0}/\rho_{ab}$ and $\Delta\rho_{c,0}/\rho_c$ correspond to the experimentally measured $\Delta\rho_{ab}/\rho_{ab}(45^\circ)$ and $\Delta\rho_c/\rho_c(90^\circ)$, respectively, since the anisotropic terms cancel for these θ values. As mentioned above and shown in Figs. 2(a) and 2(b), $\Delta\rho_{ab}/\rho_{ab}(45^\circ)$ and $\Delta\rho_c/\rho_c(90^\circ)$ contain two contributions each: a quadratic in H contribution, $\gamma_{ab}H^2$ and γ_cH^2 , respectively, and a negative contribution, $\Delta\rho_{ab}^{DW}/\rho_{ab}$ and $\Delta\rho_c^{DW}/\rho_c$, respectively. We extract two relevant quantities from the H dependence of $\Delta\rho_{ab}^{DW}/\rho_{ab}$ and $\Delta\rho_c^{DW}/\rho_c$ [see Figs. 2(a) and 2(b), respectively]: the saturation values $\Delta\rho_{ab,sat}^{DW}/\rho_{ab}$ and $\Delta\rho_{c,sat}^{DW}/\rho_c$ as well as their threshold fields $H_{ab,sat}^{DW}$ and $H_{c,sat}^{DW}$.

The T dependence of $H_{ab,sat}^{DW}$ and $H_{c,sat}^{DW}$ together with H_{SF} determined from the H dependence of $\Delta\rho_{ab,c}^{anis}/\rho_{ab,c}$ are shown in Fig. 4(a). For $T > 100 \text{ K}$, all three curves decrease linearly with increasing T , with a common T -axis intercept of $390 \pm 25 \text{ K}$. Since H_{SF} should vanish at T_N , we identify this temperature with the AF transition temperature. This determined value of T_N is in good agreement with the 382 K value of T_N extracted from the phase diagram of $\text{YBa}_2\text{Cu}_3\text{O}_x$ for this same stoichiometry.²⁷

The T dependences of the saturation values $\Delta\rho_{ab,sat}^{DW}/\rho_{ab}$ and $\Delta\rho_{c,sat}^{DW}/\rho_c$ are shown in Fig. 4(b). The in-plane data follow a power-law dependence of the form $\Delta\rho_{ab,sat}^{DW}/\rho_{ab} = \text{const} \times (1 - T/T_{ab})^\alpha$, with the best fit for $T_{ab} = 393 \text{ K}$ and $\alpha = 3.75$ (solid line in the figure). This characteristic temperature is again close to T_N , indicating that $\Delta\rho_{ab,sat}^{DW}/\rho_{ab}$ also vanishes at $T > T_N$. A similar T dependence is also characteristic to $\Delta\rho_{c,sat}^{DW}/\rho_c$ for $T > 100 \text{ K}$, as evidenced by the scaling between $\Delta\rho_{ab,sat}^{DW}/\rho_{ab}$ and $\Delta\rho_{c,sat}^{DW}/\rho_c$ shown in Fig. 4(b).

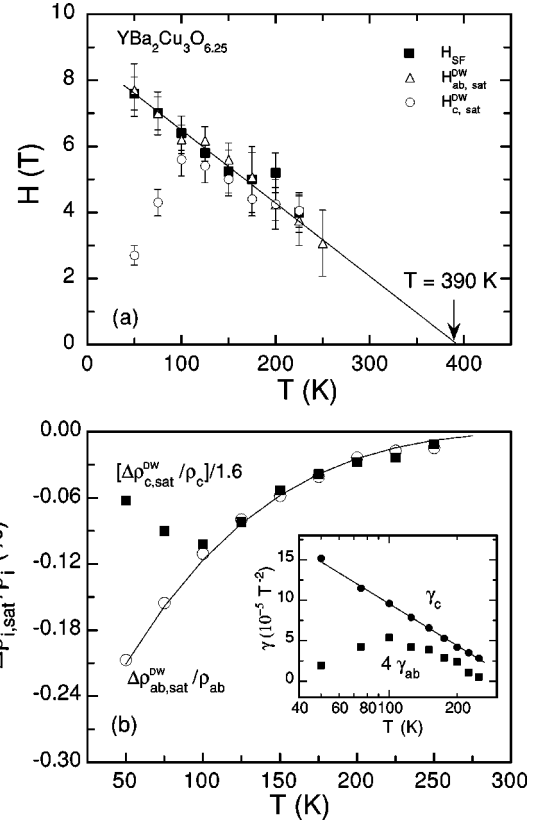


FIG. 4. (a) Temperature T dependence of the saturation fields H_{SF} , $H_{ab,sat}^{DW}$, and $H_{c,sat}^{DW}$ of $\text{YBa}_2\text{Cu}_3\text{O}_{6.25}$ single crystal. (b) Temperature T dependences of the saturation values $\Delta\rho_{ab,sat}^{DW}/\rho_{ab}$ and $\Delta\rho_{c,sat}^{DW}/\rho_c$. Inset: Temperature T dependences of the coefficients $\gamma_{ab,c}$ of the quadratic in H contributions to magnetoresistivities.

The scaling of $\Delta\rho_{ab,sat}^{DW}/\rho_{ab}$ and $\Delta\rho_{c,sat}^{DW}/\rho_c$ as well as the nearly identical values of the saturation fields $H_{i,sat}^{DW}$ ($i = ab, c$) [Fig. 4(a)] for $T > 100 \text{ K}$ are a strong indication that the same mechanism, which becomes active in the AF regime, is responsible for both $\Delta\rho_{ab}^{DW}/\rho_{ab}$ and $\Delta\rho_c^{DW}/\rho_c$ at high T . The peculiar H dependences of $\Delta\rho_{ab}^{DW}(H)$ and $\Delta\rho_c^{DW}(H)$ with their rapid decrease with increasing H for low H and their saturation at high H support the idea that the mechanism responsible for these MR terms involves the H -dependent AF domain structure. This mechanism is most likely related to scattering of the charge carriers on the AF domain walls. This scattering process occurs as a result of carrier spin relaxation on the local rotated magnetic moments within the domain wall. A similar domain-wall scattering was predicted and experimentally investigated in the case of ferromagnetic materials.^{28,29} Magnetic fields higher than H_{SF} erase the domains, the local magnetic moments acquire the same orientation, and scattering events are no longer present. Hence, the domain-wall resistance vanishes and $\Delta\rho_{ab,c}^{DW}/\rho_{ab,c}(H)$ saturates at a value that reflects the relative contribution of the DW scattering to the total resistivities. The downturn of $H_{c,sat}^{DW}$ at $T \approx 100 \text{ K}$ is, however, intriguing and might signal a change in the way the Cu spins couple with H . This change appears to be relevant to the out-of-plane transport while leaving the in-plane transport unaf-

fects ($H_{ab,sat}^{DW}$ continues to monotonically increase with decreasing T).

The H^2 coefficients $\gamma_{ab,c}$ extracted from our data have positive values over the whole measured T range, with γ_c approximately one order of magnitude larger than γ_{ab} . The T dependences of γ_{ab} and γ_c are shown in the inset to Fig. 4(b). The coefficient γ_c decreases monotonically with increasing temperature while γ_{ab} is nonmonotonic with a maximum at ≈ 100 K. For $50 \leq T \leq 250$ K, γ_c has the following logarithmic T dependence:

$$\gamma_c = 735 \times 10^{-7} \ln \frac{T^*}{T}, \quad (15)$$

with the fitting parameter $T^* = 363$ K. This value of T^* is close to the 382 K value of T_N extracted from the phase diagram of $\text{YBa}_2\text{Cu}_3\text{O}_x$ for this same stoichiometry.²⁷ This suggests that the H^2 term of $\Delta\rho_c/\rho_c$ correlates with the presence of antiferromagnetic ordering, as was previously reported on $\text{YBa}_2\text{Cu}_3\text{O}_x$ single crystals with similar oxygen content.³⁰

VI. SUMMARY

We performed simultaneous in-plane and out-of-plane magnetoresistivity measurements on antiferromagnetic $\text{YBa}_2\text{Cu}_3\text{O}_{6.25}$ single crystals in magnetic fields applied par-

allel to the ab plane. Both $\Delta\rho_{ab}/\rho_{ab}$ and $\Delta\rho_c/\rho_c$ are a superposition of three contributions.

(i) The first contribution is anisotropic, changes strongly with H for low H , and saturates at H above a certain value H_{SF} . This contribution exhibits a twofold angular symmetry for $\Delta\rho_{ab}/\rho_{ab}$ and a fourfold angular symmetry for $\Delta\rho_c/\rho_c$ upon in-plane magnetic-field rotation. We have shown that this anisotropic contribution is a result of the coupling between the antiferromagnetically ordered Cu(2) spins and the crystal lattice.

(ii) The next two contributions are isotropic. One contribution is negative and saturates at fields higher than a threshold field $H_{i,sat}^{DW}$ ($i=c,ab$). We ascribe this contribution to charge-carrier scattering on the AF domain walls. The other contribution is quadratic in H and much larger for the out-of-plane MR than for the in-plane MR. There are indications that this contribution might be due to AF ordering, although further evidence is necessary for a conclusive identification of this mechanism.

ACKNOWLEDGMENTS

This research was supported by the National Science Foundation under Grant No. DMR-0102415 at KSU and the U.S. Department of Energy under Contract No. W-31-109-ENG-38 at ANL.

*Permanent Address: National Institute of Materials Physics, R76900 Bucharest, Romania.

¹Yoichi Ando, A.N. Lavrov, and Kouji Segawa, Phys. Rev. Lett. **83**, 2813 (1999).

²E. Cimpoiasu, C.C. Almasan, A.P. Paulikas, and B.W. Veal, Physica C **364-365**, 399 (2001).

³A. Janossy, F. Simon, and T. Feher, Phys. Rev. Lett. **85**, 474 (2000).

⁴A.S. Moskvina and Yu.D. Panov, cond-mat/0008035 (unpublished).

⁵C.N. Jiang, A.R. Boldwin, G.A. Levin, T. Stein, C.C. Almasan, D.A. Gajewski, S.H. Han, and M.B. Maple, Phys. Rev. B **55**, R3390 (1997).

⁶A. Janossy, F. Simon, T. Feher, A. Rockenbauer, L. Korecz, C. Chen, A.J.S. Chowdbury, and J.W. Hodby, Phys. Rev. B **59**, 1176 (1999).

⁷B.W. Veal, H. You, A.P. Paulikas, H. Shi, Y. Fang, and J.W. Downey, Phys. Rev. B **42**, 4770 (1990).

⁸G.A. Levin, T. Stein, C.N. Jiang, C.C. Almasan, D.A. Gajewski, S.H. Han, and M.B. Maple, Physica C **282-284**, 1147 (1997).

⁹E. Cimpoiasu, G.A. Levin, C.C. Almasan, Hong Zheng, and B.W. Veal, Phys. Rev. B **63**, 104515 (2001).

¹⁰V. Sandu, E. Cimpoiasu, C. C. Almasan, A. P. Paulikas, and B. W. Veal, Proceedings of Physical Phenomena at High Magnetic Fields - IV (unpublished).

¹¹A.N. Lavrov and L.P. Kozeeva, Physica C **248**, 365 (1995).

¹²J.W. Lynn, in *Physical and Material Properties of High Temperature Superconductors*, edited by S.K. Malik and S.S. Shah (Nova Science, New York, 1994), p. 243.

¹³L. D. Landau and E.M. Lifshitz, *Theory of Elasticity*, 3rd ed.

(Pergamon Press, New York, 1986).

¹⁴U. Welp, M. Grimsditch, S. Fleshler, W. Nessler, J. Downey, G.W. Crabtree, and J. Guimpel, Phys. Rev. Lett. **69**, 2130 (1992).

¹⁵S.W. Tozer, J.L. Koston, and E.M. McCarron III, Phys. Rev. B **47**, 8089 (1993).

¹⁶V.N. Kachinsky, V.N. Kochetkov, I.N. Makarenko, V.N. Narozhnyi, and T.G. Uvarova, Physica C **247**, 347 (1995).

¹⁷D.D. Balla, A.V. Bondareko, R.V. Vovk, M.A. Obolenski, and A.A. Prodan, Low Temp. Phys. **23**, 777 (1997).

¹⁸J.D. Jorgensen, Shiyong Pei, P. Lightfoot, D.G. Hinks, B.W. Veal, B. Babrowski, A.P. Paulikas, and R. Kleb, Physica C **171**, 93 (1990).

¹⁹V.A. Kostylev, A.I. Ponomarev, N.M. Chebotaev, and S.V. Naumov, Physica C **208**, 189 (1993).

²⁰K. Yoshida, A.I. Rykov, S. Tajima, and I. Terasaki, Phys. Rev. B **60**, R15 035 (1999).

²¹J. S. Schilling and S. Klotz, in *Physical Properties of High Temperature Superconductors III*, edited by D.M. Ginsberg, (World Scientific, Singapore, 1992).

²²N. Tanahashi, Y. Iye, T. Tamegai, C. Murayama, N. Mōri, S. Yomo, N. Okazaki, and K. Kitazawa, Jpn. J. Appl. Phys., Part 2 **23**, L762 (1989).

²³M.M. Farztdinov, *Fizika Magnitnykh Domenov v Antiferromagnetikakh i Ferritakh* (Nauka, Moscow, 1981), p. 16.

²⁴A.K. Zvezdin, A.M. Kadomtseva, A.A. Kovalev, M.D. Kuz'min, L.I. Leonyk, H.I. Leonyk, A.S. Markosyan, and V.N. Milov, JETP Lett. **51**, 196 (1990).

²⁵Z.A. Kazei, N.P. Kolmakova, I.B. Krynetskii, R.Z. Levitin, and V.V. Snegirev, Physica C **185-189**, 927 (1991).

²⁶The value of H_E is large and can be estimated from $M_s H_E = k_B T_N$. Assuming $T_N \approx 400$ K and $M_s \approx 0.6 \mu_B$, we obtain $H_E \approx 600$ T.

- ²⁷J.M. Tranquada, A.H. Moudden, A.I. Goldman, P. Zolliker, D.E. Cox, G. Shirane, S.K. Sinha, D. Vaknin, D.C. Johnston, M.S. Alvarez, A.J. Jacobson, J.T. Lwwandowski, and J.M. Newsam, Phys. Rev. B **38**, 2477 (1988).
- ²⁸P.M. Levy and S. Zhang, Phys. Rev. Lett. **79**, 5110 (1997).
- ²⁹A. Braats, G. Tara, and G.E.W. Bauer, Phys. Rev. B **60**, 3406 (1999).
- ³⁰A.N. Lavrov, Yoichi Ando, Kouji Segawa, and J. Takeya, Phys. Rev. Lett. **83**, 1419 (1999).